

# Machine Learning Framework for Catalytic Activity Predictions of Transition Metal Sulfides for the Oxygen Reduction Reaction

Dilip Krishnamurthy (dkrishn1),  
Nathan Nakamura (nnakamur), Nikhil Rajeev (nrajeev),  
Phil Smith (philsmits)

December 11, 2018

## Abstract

*Computational screening studies to discover promising catalyst materials are designed to identify candidates which exhibit optimal adsorption characteristics with respect to a key reaction intermediate ( $\Delta G_{OH^*}$  for the oxygen reduction reaction). The local coordination environment across heterogeneous surfaces has been found to strongly impact the resultant adsorption strength. Currently, time-consuming density functional theory (DFT) calculations are generally used to predict  $\Delta G_{OH^*}$ , limiting the structural and compositional space that can be explored with regards to candidate catalyst materials. Here, we explore the use of various machine learning algorithms and neural networks to develop a universal model describing  $\Delta G_{OH^*}$  on transition metal sulfide surfaces. We explore several features in addition to the coordination environment and find that K-Nearest Neighbor models and a simple neural net performed best, giving root-mean-squared error values ( $\approx 0.16$  eV) on the predicted  $\Delta G_{OH^*}$  similar to those obtainable via DFT calculations. We highlight that the presented approach based on geometric features of the catalyst surface site—based on merely counting nearest neighbor atoms—can lead to high fidelity activity predictions comparable to that of DFT.*

## 1 Introduction

Current efforts in materials design and discovery are based on experimental observations and computational simulations, both of which are heavy time and resource-dependent processes. Many materials for energy storage and conversion devices are approaching their theoretical limit. For example, battery anode and cathode materials

are near their theoretical energy density limit,[7, 34, 22, 39] and similarly fuel cell catalysts are approaching their efficiency limits that are imposed by scaling relations between the reaction intermediates.[30, 38, 1, 36] The process of material discovery is rather slow with high fidelity DFT computation, which can be enhanced through the use of machine learning and artificial intelligence models which can sift through large datasets and predict optimal materials for a given application in a fraction of the time. Catalyst materials, particularly materials to enhance the oxygen reduction reaction (ORR) that occurs in fuel cells, represent an attractive candidate to explore machine learning approaches in materials prediction and discovery.

Over the past decade, breakthroughs have occurred in catalyst discovery through heavy first-principles computation. A good heterogeneous catalyst for a given chemical reaction very often has only a few specific types of surface sites that are catalytically active. Widespread methodologies such as Sabatier-type activity plots determine optimal adsorption energies to maximize catalytic activity, but these are difficult to use as guidelines to devise new catalysts. Additionally, it has been shown that the variation in adsorption strength across heterogeneous surface sites is strongly dependent on the local environment, especially in metallic systems. Therefore, there is a huge potential to accelerate materials discovery if common geometric features associated with the local atomic environment of highly active catalytic sites can be identified. This will allow us to invert the design problem and formulate the material search as merely finding the optimal local atomic environment to maximize catalytic activity, rather than requiring computationally expensive first-principles calculations.

Herein, we identify atomic structure-catalytic activity relationships for the case study of materials design for an ORR reaction using different classes of transition metal sulfides  $M_xS_y$ , where M represents a metal cation and S represents a sulfur atom. The rich phase diagram of metal sulfides provide the opportunity to explore various compositions and atomic coordination environments. The classes of materials studied in this report include Ni<sub>x</sub>S,[47] Co<sub>x</sub>S, Cr<sub>x</sub>S, Cu<sub>x</sub>S, Mn<sub>x</sub>S, Mo<sub>x</sub>S, V<sub>x</sub>S, Ru<sub>x</sub>S and Sc<sub>x</sub>S, with various compositions  $M_xS_y$  explored for each class. Catalytic activity is described by an adsorption energy  $\Delta G_{OH^*}$ , which represents the binding strength of the OH\* group to a specific site on a metal sulfide surface (Figure 1). The  $\Delta G_{OH^*}$  has previously been found to be a suitable descriptor of catalytic activity in ORR reactions. By exploring various machine learning and neural network-based techniques, we find that a universal model to link coordination environment to catalytic activity across transition metal sulfide classes is achievable. We learn geometric features and construct a robust machine learning model for  $\Delta G_{OH^*}$  prediction, and find that predicted root-mean-squared error (RMSE) values of the models are comparable to RMSE values for  $\Delta G_{OH^*}$  from first-principles calculations.

## 2 Methods

### 2.1 Data and Featurization

The training dataset was gathered by team member Dilip Krishnamurthy over the last couple of years via his thesis research, and consists of catalytic activity values ( $\Delta G_{OH^*}$ ) obtained from density functional theory (DFT) calculations for a variety of transition metal sulfide classes. The DFT simulations leveraged error-estimation capabilities to increase the robustness of predictions<sup>3,4</sup> in identifying highly-active materials that better match experimental activity. The result of this is that rather than obtaining a single  $\Delta G_{OH^*}$  value from a DFT calculation, a Gaussian distribution of  $\Delta G_{OH^*}$  values are obtained (Figure 2a).

To featurize the dataset and apply appropriate  $\Delta G_{OH^*}$  labels, three steps were taken. First, each  $\Delta G_{OH^*}$  in the distribution is assigned to its corresponding  $M_xS_y$  structure and binding site. Next, the nearest neighbor atoms to that binding site is determined using a Voronoi approach for the first and second coordination shells (Figure 2b). The Voronoi diagram perpendicularly bisects the distance between neighboring atoms, allowing nearest neighbor and second nearest neighbor atoms to be determined by simply counting the sides of the resultant shape formed around the reference atom. Lastly, the atoms electronegativity and atomic number is inserted into the feature matrix. Each featurization resulted in an 18x3 matrix, due to the 3 descriptors (electronegativity, coordination number, and atomic number) and the 9 potential atom types in each coordination shell (Figure 2c). Since we use 2 coordination shells (i.e., out to the second nearest neighbor), the total height of the matrix is 18. The total size of the final dataset was N=1470.

### 2.2 Approach

We construct robust machine learning models by utilizing error-estimation capabilities[46] within the BEEF-vdW exchange correlation functional while generating DFT data of adsorption characteristics.[29, 35, 37, 19, 3, 10, 15, 16, 42, 32]

In order to understand the importance of each feature considered in this work—coordination numbers of nearest and next nearest shells—, we first construct linear regression models. Subsequently, we explore several machine learning approaches[24, 49, 25, 21, 31, 17, 20, 28, 27, 43, 18, 4, 44, 45, 33, 9, 14] including k-nearest-neighbors regression, support vector regressor, decision tree regressor and neural network. We report promising models in the results section. Various machine learning models, along with neural networks were tested to ensure that the most viable approach was selected. The machine learning approaches explored include, K-nearest neighbors (KNN) regression, radius nearest neighbors (RNN) regression and support vector machine (SVM) regression. The resultant RMSE and MAE values for each of these, along with our neural network, are shown in Table 1 and compared with the accuracy from [40]. It's clear that the KNN regressor and our neural network provide the best results, and as such they are described in more detail in the Results section.

Additional to featurizing the data, using multiple analysis we conclude that the normalized  $\Delta G_{OH^*}$  vector provided the highest accuracy. However, it is worth noting that normalizing the input feature matrix did not have an impact on the overall performance. This is due to the highly nonlinear nature of the  $\Delta G_{OH^*}$  values.

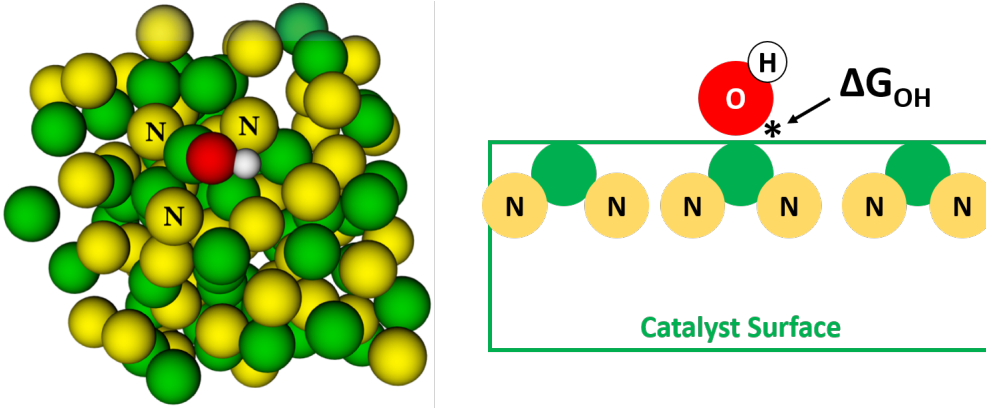


Figure 1: Structure file for a surface showing the adsorption site as a metal atom (green) and the three nearest neighbor (represented using the letter N) sulfur atoms (yellow). Red is used to indicate the oxygen atom and white is used for hydrogen, which together represent the  $\text{OH}^*$  adsorbate.  $\Delta G_{\text{OH}^*}$  corresponds to the strength of adsorption to the catalyst surface.

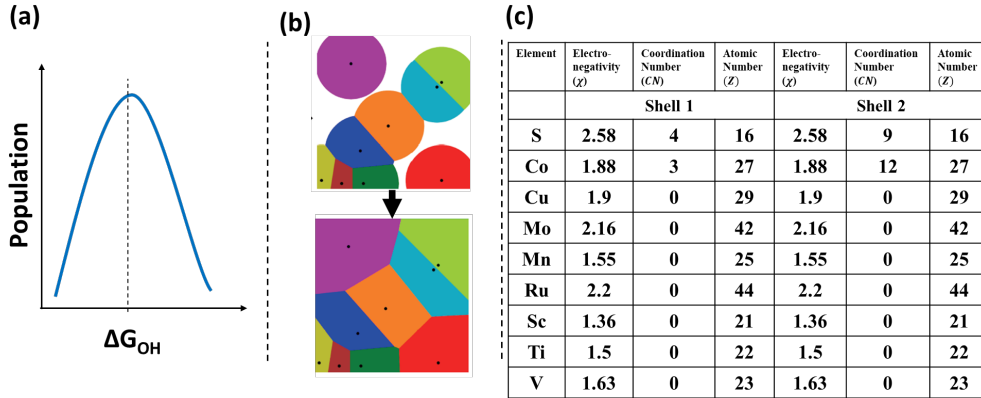


Figure 2: (a) Example Gaussian distribution of  $\Delta G_{\text{OH}^*}$  values obtained from DFT simulations. (b) Voronoi diagram to predict 1<sup>st</sup> and 2<sup>nd</sup> coordination shells around a reference atom. Atoms are depicted by black dots. The colored spheres surrounding each atom grow outward until they all contact each other. The resultant number of distinct sides on each shape represents the amount of nearest neighbors for that atom. (c) Example features matrix, shown for a CoS surface.

### 3 Results

The table below summarizes the accuracy values of select machine learning approaches.

Method	RMSE	MAE
<b>k Nearest Neighbours</b>	0.229	0.171
Radius Nearest Neighbours	0.258	0.198
<b>Neural Network</b>	0.224	0.169
Decision Tree Regressor	0.31	0.19
Support Vector Regressor	1.45	1.16

### 3.1 Linear Models

In order to understand the importance of each feature considered in this work—coordination numbers of nearest and next nearest shells—, we first construct linear regression models and find that the coordination numbers play the most significant role in determining the accuracy.

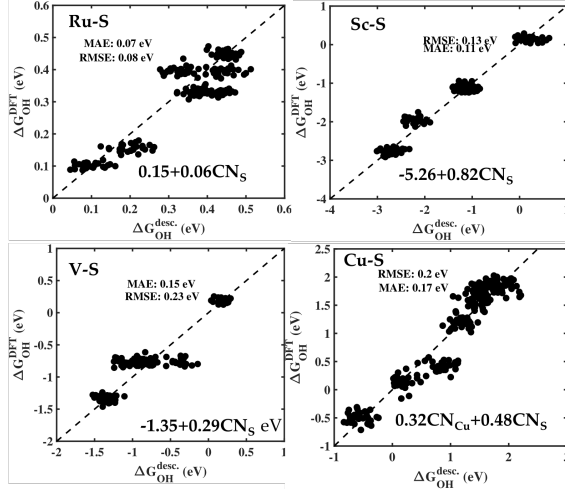


Figure 3: Understanding the importance of the coordination environment through the use of simple linear models for each transition metal sulfide class separately. We find that although the RMSE/MAE is promising for each individual class, an attempt to construct a universal model for the entire transition metal sulfide class fails ( $RMSE > 0.35$  eV). Therefore, we explore several machine learning models.

### 3.2 Support Vector Regressor and Decision Tree Regressor

Support vector regressor(SVR) and decision tree regressor performance in this work is inferior to the error accuracy provided by KNN algorithm and RNN regression methods. This can be attributed to the known success of nearest neighbour methods on regression tasks [6]. However, in this study the superior performance of KNN regressor can be due to the Voronoi shaped non linear decision boundaries used by KNN being inline with the input data, where one of the key features is estimated using Voronoi tessellation. Decision trees classify new records

based independent of neighboring records, creating an inferior performance in the presence of smaller training data set [13]. This can be considered as the reason for the comparatively poor performance of decision tree regressor. SVR which uses polynomial feature kernel fails to learn the non linear fit, thereby creating the worst performance among all the methods tested. However, with an increase in training samples the accuracy of SVR is expected to increase.

### 3.3 KNN Regression

In using k-nearest neighbor, regression is chosen since we want to predict an actual number for  $\Delta G_{OH}$ . The distinct quality of k-nearest neighbors over other algorithms is that they classify the data without building the model first [8]. This case based explanation is advantageous in situations where black-box models are inadequate [11]. For determining the optimal number of neighbors or k-value to use in the algorithm, we look at the resulting MAE for k ranging from 0 to 100. The resulting elbow curve is shown in Figure 4. From this plot, the optimal k-value is 17. After training the algorithm, we obtain a low MAE of 0.171, RMSE of 0.229, standard deviation of 0.22 and  $R^2$  value of 0.936 for our test data. Figure 5 shows the  $\Delta G_{OH}$  from DFT calculations vs KNN prediction which are really close to the dotted y=x line.

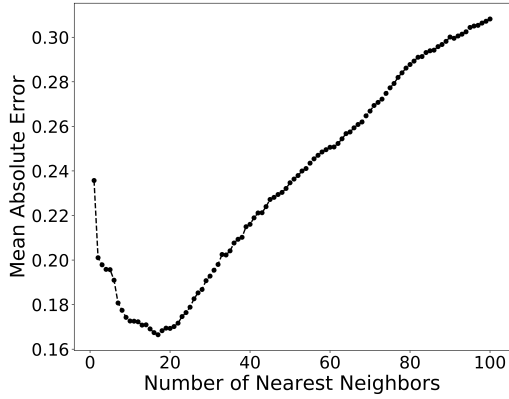


Figure 4: Mean squared error vs number of nearest neighbors

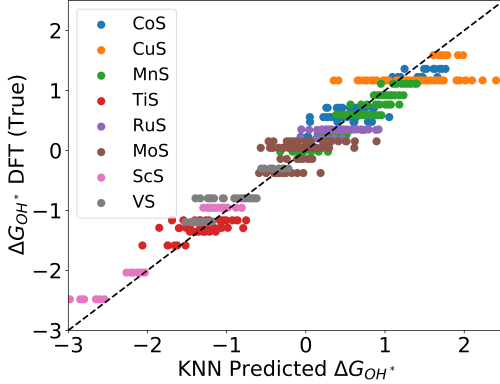


Figure 5:  $\Delta G_{OH}$  from DFT calculation vs KNN prediction

### 3.4 Neural Network

A neural network system is trained to predict the  $\Delta G_{OH}$  values. With adequate training, the model achieves an RMSE value of 0.278 and MAE of 0.217 on the test data. The neural network has 5,941 parameters and 108 neurons, containing 2 hidden layers with ReLU activation function. Since overtraining a neural network leads to losing its ability to generalize on data [2], due to overfitting, the number of training epochs required is tested and adjusted by using early stopping, after analysing the error as a function of epochs, as illustrated in Figure 6. Additional to preventing overfitting due to overtraining by using early stopping, as a general trend the bias falls and variance increases with number of hidden units [12]. Therefore, the number of layers required to prevent overfitting and provide a good fit model is tested, and concluded to be two. Further increase in layers has no role in improving the test accuracy, and contributed slightly towards increasing the variance.

It can be noted from the Figure 7, that the accuracy obtained from DFT calculations vs neural network is very close to the  $y=x$  line indicating a very good performance by the model. However, this performance is very similar to the trend observed while using kNN algorithm. The primary advantage of kNN implementation is the good generalization capability with limited training samples. However, with 5,941 parameters and additional hyperparameters the performance of a Neural Network is limited by the number of training data points. A larger data

dataset will provide a better test accuracy with NN. Due to large computational expense of performing DFT calculations the training data set size currently available for this study is limited. As an extension to this work, more data points from further DFT studies can be added to the training set, helping the Neural Network learn better. Since, the current Neural Network model with limited data points is providing an accuracy similar to DFT studies, it is expected that a larger training set will provide a model that could be a very promising alternative to first principle methods currently available.

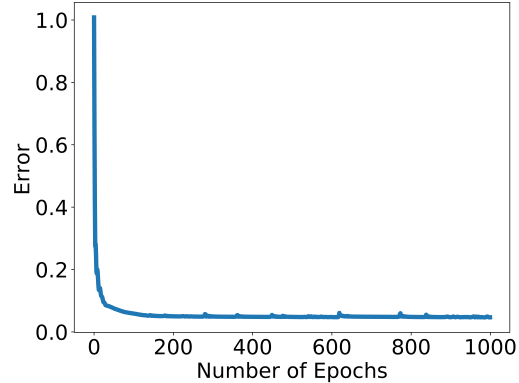


Figure 6: Loss vs Epoch

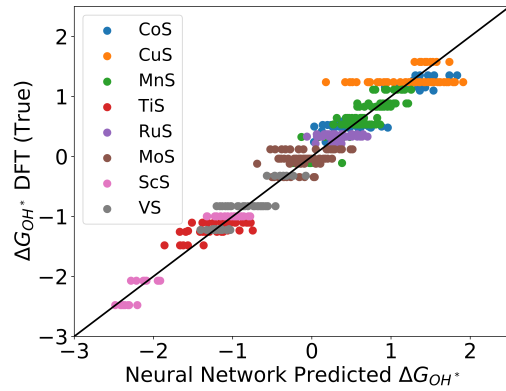


Figure 7:  $\Delta G_{OH}$  from DFT calculation vs Neural Network prediction

### 3.5 KNN for $\Delta G_{OH}$ prediction for individual metal-sulfide classes

For assessing the performance of the universal transition metal sulphide  $\Delta G_{OH}$  predictor discussed in this report and understand the transition metal sulphides with most difficulty in modeling, RMSE and MAE disparity plots were developed using individual KNN and Neural Network models for each of the eight metal sulphides discussed in this report. The Figure 7 shows that the KNN model used for predicting the  $\Delta G_{OH}$  for CuS has the highest RMSE and MAE values (0.37 and 0.48). The disparity plot obtained for Neural Net shows a very similar trend, thereby making it evident that removing CuS from the training data can provide a better prediction accuracy for  $\Delta G_{OH}$  for other transition metal sulphides. This provides an insight on the compounds that can be combined together for creating a more accurate  $\Delta G_{OH}$  prediction model.

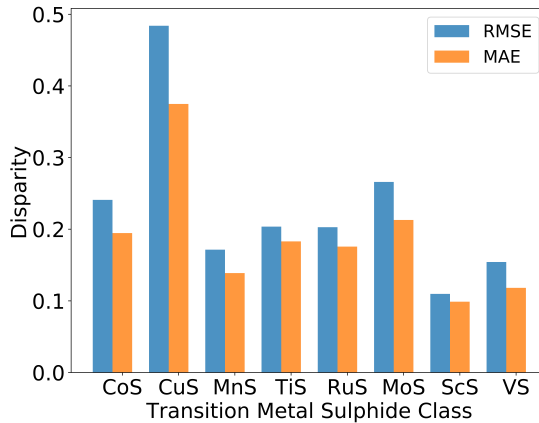


Figure 8: RMSE / MAE disparity plot

## 4 Discussion on Results and Comparison to Prior Literature

Thus far, such geometric or atomic coordination-based approaches to predict bonding activity have been established for metal surfaces[5] and metal nanocatalysts[23]. Additionally, a prior study predicting energies of intermetallics (metal alloys) used a genetic algorithm-based

machine learning approach to achieve accuracies similar to those achieved in this report[40]. The accuracy values reported in these prior works are compared to those found in our work (Table 1). The RMSE reported in this work is comparable to DFT accuracy (Accuracy of the scale of 0.15 eV MAE from earlier works by Medford et al., the Viswanathan group, etc [26, 42, 19]) indicating that the same level of fidelity is possible based on a geometric descriptor with orders of magnitude improvement in the computational cost and time. This indicates that we are on the right trajectory for rapid materials screening without the use of first-principles calculations.

As mentioned before, identification of simple structure-energy-activity descriptors using machine learning allows for rapid identification of candidate materials and can accelerate the discovery of electrocatalysts for ORR. Among the multiple machine learning models analyzed (Table 2), it is noted that the RMSE and MAE values provided by KNN and Neural Network is the lowest, with RNN providing a slight higher error. Polynomial fit of SVR does not provide a good approximation of the highly non linear training data, thereby failing with high RMSE and MAE values. This can be clearly understood from the non linear nature of data we are training. The RMSE values obtained from KNN and Neural Network is comparable to earlier work by Medford et al., the Viswanathan group, etc [26, 42, 19]), indicating very promising results.

As mentioned above, KNN and Neural Network provides an accuracy similar to DFT results. The unique ability of artificial neural network adapt and being able to model non linearity and arbitrary functions mapping make it quite useful in predicting the  $\Delta G_{OH}$  values. However, there are many factors that affect the performance of these neural networks, for which no systematic investigation has been done yet. The trial and error approach for the hyperparameter tuning can lead to inconsistency in results obtained. This can be attributed to the black box model of neural network, where no explicit relationship between input and output can be studied [48]. This difficulty in interpreting the results from the network can be challenging in physics based models as the one discussed in this paper.

However, some of the disadvantages of neural network is not inherited by other machine learning models available. The large number of parameters and hyperparameters that require tuning in a neural network is not present in other machine learning models, such as KNN or RNN discussed in this paper. Therefore, these models can provide a good estimate of the  $\Delta G_{OH}$  value predictions with a smaller dataset. Given the non linear nature

of the data available for prediction, it can be clearly seen from Table 2 that the non linear classifiers such as KNN performs very well. The locally weighted linear segments of KNN classifier can model complex shapes given the appropriate number of nearest neighbours. However, the ability for KNN to model non linearity is limited by the nature of the algorithm and therefore its ability to provide more accurate predictions with a larger dataset is questionable.

The advantages of both KNN and NN include automatically calculated decision boundary in the KNN case and automatically calculated weights in the NN case. They both also allow incremental learning, meaning that the performance can be incrementally improved when new training data are added to the existing training data. In our case, although our data set is small, we were able to find the optimal k-value which could have been difficult to find for a data set of this size. This small data set is also the reason that KNN and NN performed in similar manner, since NN typically require a large data set. However, we see that the MAE and RMSE from the NN predictions are relatively small, as a result NN one of the most viable option available. Also, the computational complexity of kNN did not present itself as an issue for us.

In light of the limitations and advantages of the models discussed above, neural network offers a number of advantages, including the ability to detect complex non-linear relationships between dependent and independent variable and its ability to detect interactions between the predictor variables in the availability of a large training dataset [41]. While the advantages of the method is being limited by the black box nature of the algorithm, given the literature and research in this field is expanding, this bottleneck might be soon circumvented by new findings. Even though the capability and ability for machine learning models to replace DFT analysis is currently arguable, the machine learning models discussed in the paper can provide the first basis for selecting materials for further DFT studies, and thereby eventually allow for rapid screening within different material classes for a variety of reactions.

## 5 Conclusion

Here, we utilize simple geometric descriptors to effectively predict how atomic structure and binding site affect adsorption energy ( $\Delta G_{OH^*}$ ) in transition metal sulfide catalyst materials. The geometric-descriptor-based approach can be used to computationally efficiently identify op-

timal material candidates for a wide range of electrochemical systems. We find that a KNN regressor and neural network provide the best results, with RMSE values falling within the range of RMSE for  $\Delta G_{OH^*}$  values predicted by time-consuming first-principles calculations. We propose to explore other potentially important features such as higher shell coordination and encoding information about the adsorbate atom on the catalyst. In addition, we will rationalize the coefficients in our high-accuracy models based on the trends in (i) the metal-metal bonding strength, (ii) the atomic-scale distances around the active site, and (iii) the metal-sulfur bonding strength, for each transition metal sulfide class. We will subsequently include mixed transition metal sulfides (stoichiometry given by  $M_1x_1M_2x_2..M_nx_nS_y$ ) into our dataset and determine the efficacy of the current approach, which is a natural extension within the constructed universal feature matrix.

## 6 Data Availability

The code used to perform his work is available at this Github Profile

## References

- [1] Frank Abild-Pedersen, Jeff Greeley, Felix Studt, Jan Rossmeisl, TR Munter, Poul Georg Moses, Egill Skulason, Thomas Bligaard, and Jens Kehlet Nørskov. Scaling properties of adsorption energies for hydrogen-containing molecules on transition-metal surfaces. *Phys. Rev. Lett.*, 99(1):016105, 2007.
- [2] S Agatonovic-Kustrin and R Beresford. Basic concepts of artificial neural networks (ann) modeling and its application in pharmaceutical research. *Journal of Pharmaceutical and Biomedical Analysis*, 22(5):717 – 727, 2000.
- [3] Zeeshan Ahmad and Venkatasubramanian Viswanathan. Quantification of uncertainty in first-principles predicted mechanical properties of solids: Application to solid ion conductors. *Phys. Rev. B*, 94(6):064105, 2016.
- [4] Prasanna V Balachandran, Antoine A Emery, James E Gubernatis, Turab Lookman, Chris Wolverton, and Alex Zunger. Predictions of new ab o 3 perovskite compounds by combining machine learning and density functional theory. *Physical Review Materials*, 2(4):043802, 2018.
- [5] Federico Calle-Vallejo, David Loffreda, Marc TM Koper, and Philippe Sauvet. Introducing structural sensitivity into adsorption-energy scaling relations by means of coordination numbers. *Nature chemistry*, 7(5):403, 2015.
- [6] George H. Chen and Devavrat Shah. Explaining the success of nearest neighbor methods in prediction. *Foundations and Trends® in Machine Learning*, 10(5-6):337–588, 2018.
- [7] Jang Wook Choi and Doron Aurbach. Promise and reality of post-lithium-ion batteries with high energy densities. *Nat. Rev. Mater.*, 1(4):16013, 2016.
- [8] B Dasarathy. Nearest neighbor pattern classification techniques ieee computer society press. *Silver Spring, MD*, 1991.
- [9] Brian DeCost, Jason Hattrick-Simpers, Yangang Liang, Ichiro Takeuchi, and Aaron Kusne. Active machine learning for combinatorial exploration of metal-insulator transitions. *Bull. Am. Phys. Soc.*, 2018.
- [10] Siddharth Deshpande, John R. Kitchin, and Venkatasubramanian Viswanathan. Quantifying uncertainty in activity volcano relationships for oxygen reduction reaction. *ACS Catal.*, 6(8):5251–5259, 2016.
- [11] Stephan Dreiseitl and Lucila Ohno-Machado. Logistic regression and artificial neural network classification models: a methodology review. *Journal of Biomedical Informatics*, 35(5):352 – 359, 2002.

- [12] Stuart Geman, Elie Bienenstock, and René Doursat. Neural networks and the bias/variance dilemma. *Neural Computation*, 4(1):1–58, 1992.
- [13] Peter Harrington. Machine learning in action. *Shelter Island, NY: Manning Publications Co*, 2012.
- [14] Jason R Hattrick-Simpers, Kamal Choudhary, and Claudio Cognale. A simple constrained machine learning model for predicting high-pressure-hydrogen-compressor materials. *Mol. Syst. Des. Eng.*, 2018.
- [15] Gregory Houchins and Venkatasubramanian Viswanathan. Quantifying confidence in density functional theory predictions of magnetic ground states. *Phys. Rev. B*, 96(13):134426, 2017.
- [16] Gregory Houchins and Venkatasubramanian Viswanathan. Towards ultra-low cobalt cathodes: A high fidelity phase search incorporating uncertainty quantification of li-ni-mn-co oxides. *arXiv:1805.08171 [cond-mat.mtrl-sci]*, 2018.
- [17] Maxwell Hutchinson, Erin Antono, Brenna Gibbons, Sean Paradiso, Julia Ling, and Bryce Meredig. Solving industrial materials problems by using machine learning across diverse computational and experimental data. *Bull. Am. Phys. Soc.*, 2018.
- [18] Kyoungdoc Kim, Logan Ward, Jiangang He, Amar Krishna, Ankit Agrawal, Peter Voorhees, and Christopher Wolverton. Accelerated discovery of quaternary heusler with high-throughput density functional theory and machine learning. *Bull. Am. Phys. Soc.*, 2018.
- [19] Dilip Krishnamurthy, Vaidish Sumaria, and Venkatasubramanian Viswanathan. Maximal predictability approach for identifying the right descriptors for electrocatalytic reactions. *J. Phys. Chem. Lett.*, 9(3):588–595, 2018.
- [20] Julia Ling, Erin Antono, Saurabh Bajaj, Sean Paradiso, Maxwell Hutchinson, Bryce Meredig, and Brenna M Gibbons. Machine learning for alloy composition and process optimization. In *ASME Turbo Expo 2018: Turbomachinery Technical Conference and Exposition*, pages V006T24A005–V006T24A005. American Society of Mechanical Engineers, 2018.
- [21] Julia Ling, Maxwell Hutchinson, Erin Antono, Sean Paradiso, and Bryce Meredig. High-dimensional materials and process optimization using data-driven experimental design with well-calibrated uncertainty estimates. *Integr. Mater. Manuf. Innov.*, 6(3):207–217, 2017.
- [22] Alan Luntz. Beyond lithium ion batteries, 2015.
- [23] Xianfeng Ma and Hongliang Xin. Orbitalwise coordination number for predicting adsorption properties of metal nanocatalysts. *Physical review letters*, 118(3):036101, 2017.
- [24] John C Mauro. Decoding the glass genome. *Curr. Opin. Solid State Mater. Sci.*, 22(2):58–64, 2018.
- [25] John C Mauro, Adama Tandia, K Deenamma Vargheese, Yihong Z Mauro, and Morten M Smedskjaer. Accelerating the design of functional glasses through modeling. *Chem. Mater.*, 28(12):4267–4277, 2016.
- [26] Andrew J Medford, Jess Wellendorff, Aleksandra Vojvodic, Felix Studt, Frank Abild-Pedersen, Karsten W Jacobsen, Thomas Bligaard, and Jens K Nørskov. Assessing the reliability of calculated catalytic ammonia synthesis rates. *Science*, 345(6193):197–200, 2014.
- [27] Bryce Meredig, Ankit Agrawal, Scott Kirklin, James E Saal, JW Doak, Alan Thompson, Kunpeng Zhang, Alok Choudhary, and Christopher Wolverton. Combinatorial screening for new materials in unconstrained composition space with machine learning. *Phys. Rev. B*, 89(9):094104, 2014.
- [28] Bryce Meredig, Erin Antono, Carena Church, Maxwell Hutchinson, Julia Ling, Sean Paradiso, Ben Blaiszik, Ian Foster, Brenna Gibbons, Jason Hattrick-Simpers, Apurva Mehta, and Logan Ward. Can machine learning identify the next high-temperature superconductor? examining extrapolation performance for materials discovery. *Mol. Syst. Des. Eng.*, 3:819–825, 2018.
- [29] ZK Nagy and RD Braatz. Distributional uncertainty analysis using power series and polynomial chaos expansions. *J. Process Control*, 17(3):229–240, 2007.
- [30] Jens Kehlet Nørskov, Jan Rossmeisl, Ashildur Logadottir, LRKJ Lindqvist, John R Kitchin, Thomas Bligaard, and Hannes Jonsson. Origin of the overpotential for oxygen reduction at a fuel-cell cathode. *J. Phys. Chem. B*, 108(46):17886–17892, 2004.
- [31] Anton O Oliynyk, Erin Antono, Taylor D Sparks, Leila Ghadbeigi, Michael W Gaultois, Bryce Meredig, and Arthur Mar. High-throughput machine-learning-driven synthesis of full-heusler compounds. *Chem. Mater.*, 28(20):7324–7331, 2016.
- [32] Vikram Pande and Venkatasubramanian Viswanathan. Robust high-fidelity dft study of the lithium-graphite phase diagram. *Phys. Rev. Mater.*, page (accepted), 2018.
- [33] Fang Ren, Logan Ward, Travis Williams, Kevin J Laws, Christopher Wolverton, Jason Hattrick-Simpers, and Apurva Mehta. Accelerated discovery of metallic glasses through iteration of machine learning and high-throughput experiments. *Sci. Adv.*, 4(4):eaaoq1566, 2018.
- [34] Oleg Sapunkov, Vikram Pande, Abhishek Khetan, Chayanit Choomwattana, and Venkatasubramanian Viswanathan. Quantifying the promise of ‘beyond’li-ion batteries. *Transl. Mater. Res.*, 2(4):045002, 2015.
- [35] James R Stewart. Usacm thematic workshop on uncertainty quantification and data-driven modeling. Technical report, Sandia National Lab.(SNL-NM), Albuquerque, NM (United States), 2017.
- [36] Peter Strasser, Shirlaine Koh, Toyli Anniyev, Jeff Greeley, Karren More, Chengfei Yu, Zengcai Liu, Sarp Kaya, Dennis Nordlund, Hirohito Ogawa, Michael F. Toney, and Anders Nilsson. Lattice-strain control of the activity in dealloyed core-shell fuel cell catalysts. *Nat. Chem.*, 2(6):454, 2010.
- [37] Vaidish Sumaria, Dilip Krishnamurthy, and Venkatasubramanian Viswanathan. Quantifying confidence in dft predicted surface pourbaix diagrams and associated reaction pathways for chlorine evolution. *ACS Catal.*, 8:9034–9042, 2018.
- [38] Jin Suntivich, Hubert A Gasteiger, Naoaki Yabuuchi, Haruyuki Nakaniishi, John B Goodenough, and Yang Shao-Horn. Design principles for oxygen-reduction activity on perovskite oxide catalysts for fuel cells and metal-air batteries. *Nat. Chem.*, 3(7):546, 2011.
- [39] Michael M Thackeray, Christopher Wolverton, and Eric D Isaacs. Electrical energy storage for transportation—approaching the limits of, and going beyond, lithium-ion batteries. *Energy Environ. Sci.*, 5(7):7854–7863, 2012.
- [40] Kevin Tran and Zachary W Ullissi. Active learning across intermetallics to guide discovery of electrocatalysts for co 2 reduction and h 2 evolution. *Nature Catalysis*, 1(9):696, 2018.
- [41] Jack V. Tu. Advantages and disadvantages of using artificial neural networks versus logistic regression for predicting medical outcomes. *Journal of Clinical Epidemiology*, 49(11):1225 – 1231, 1996.
- [42] Olga Vinogradova, Dilip Krishnamurthy, Vikram Pande, and Venkatasubramanian Viswanathan. Quantifying confidence in dft-predicted surface pourbaix diagrams of transition-metal electrode-electrolyte interfaces. *Langmuir*, 34(41):12259–12269, 2018.
- [43] Logan Ward, Ankit Agrawal, Alok Choudhary, and Christopher Wolverton. A general-purpose machine learning framework for predicting properties of inorganic materials. *njp Computational Materials*, 2:16028, 2016.
- [44] Logan Ward, Ruoqian Liu, Amar Krishna, Vinay I Hegde, Ankit Agrawal, Alok Choudhary, and Chris Wolverton. Including crystal structure attributes in machine learning models of formation energies via voronoi tessellations. *Phys. Rev. B*, 96(2):024104, 2017.
- [45] Logan Ward, Stephanie C O’Keeffe, Joseph Stevick, Glenton R Jelbert, Muratahan Aykol, and Chris Wolverton. A machine learning approach for engineering bulk metallic glass alloys. *Acta Mater.*, 159:102–111, 2018.
- [46] Jess Wellendorff, Keld T Lundgaard, Andreas Møgelhøj, Vivien Petzold, David D Landis, Jens K Nørskov, Thomas Bligaard, and Karsten W Jacobsen. Density functionals for surface science: Exchange-correlation model development with bayesian error estimation. *Phys. Rev. B*, 85(23):235149, 2012.
- [47] Bing Yan, Dilip Krishnamurthy, Christopher H Hendon, Siddharth Deshpande, Yogesh Surendranath, and Venkatasubramanian Viswanathan. Surface restructuring of nickel sulfide generates optimally coordinated active sites for oxygen reduction catalysis. *Joule*, 1(3):600–612, 2017.
- [48] Guoqiang Zhang, B. Eddy Patuwo, and Michael Y. Hu. Forecasting with artificial neural networks: The state of the art. *International Journal of Forecasting*, 14(1):35 – 62, 1998.
- [49] Qiuju Zheng and John C Mauro. Variability in the relaxation behavior of glass: Impact of thermal history fluctuations and fragility. *J. Chem. Phys.*, 146(7):074504, 2017.